

Behaviour of concrete-filled cold-formed steel columns under axial loading

Chanchal Sonkar¹
¹Senior Scientist
Structural Engineer-
ing Group
CSIR-CBRI Roorkee
chanchalsonkar@cbri.res.in

Chanchal Sonkar, born 1988, received his civil engineering degree from Malaviya National Institute of Technology, Jaipur, Rajasthan, India. He is presently Senior Scientist at Structural Engineering Group CSIR-CBRI Roorkee. His main area of expertise is steel structures and repair/rehabilitation of distressed structures.

Mickey Mecon Dalbehera² and Ajay Chourasia³

² Principal Scientist, CSIR-Central Building Research Institute, India
Email: mickey@cbri.res.in

³ Chief Scientist, CSIR-Central Building Research Institute, India
Email: ajayc@cbri.res.in

Abstract. This paper discusses about axial performance of concrete-filled cold-formed steel columns (CFSTC). The advantages associated with these members are their high load-carrying capacity, high stiffness, large energy absorption capacity and better earthquake-resistant performance. These excellent structural performances can be ascribed to the synergistic interaction between the steel tube and concrete core; the steel tube provides confinement to the circumferential expansion of concrete core while acting as permanent formwork whereas the concrete core prevents the steel tube from buckling inward, alleviating the local buckling effect. Six specimens have been tested and the ultimate axial load-bearing capacity, load–deformation behaviour, buckling interactions and failure pattern of CFSTC columns are discussed investigated in detail. Square built-up sections by joining four U-sections with dimensions of 140 mm (web), 50 mm (flange) using self-drilling screws have been conceptualized for making CFSTC specimens using high strength 1 mm thick cold-formed steel galvanized sheet. Effect of parameters such as concrete grade and screw spacing are discussed in detail. Tests for mechanical properties of CFS and compressive strength of concrete cubes have also been conducted. CFSTC specimens demonstrated a higher load-bearing capability and ductility which may be utilized as novel techniques for strengthening deteriorated structures.

Keywords: Concrete-filled cold-formed steel columns (CFSTC), ultimate strength, buckling, load–deformation, concrete.

1 Introduction

The composite concrete-filled cold-formed steel columns (CFSTC) are utilized in many different types of structures because of their superior axial capacity. Over the past few decades, extensive studies have been carried out on CFSTC's (Shanmugam and Lakshmi (2001), Uy et al. (2011), Wang et al. (2020), Tao et al., (2013), Rahnavard et al. (2022a)). The utilization of CFSTC in construction has a number of advantages such as higher speed of construction, lesser use of formwork (for casting of concrete), less wastage, higher strength-to-weight ratio etc. (Shanmugam and Lakshmi (2001), Uy et al. (2011)). The concrete section mitigates the premature local buckling of the cold-formed steel built-up (CFSBU) tubular section and the confinement imparted by the CFSBU tubes to the concrete augments the growth of the strength of the concrete section.

Consequently, these CFSTC columns offer better fire resistance together with enhanced strength and rigidity cost-effectively in an environmentally responsible way. Also, design methodologies described by various international codal provision (AS 5100.6 (2004), AS/NZS 2327 (2004), ANSI/AISC 360-05 (2005), DBJ/T 13-51 (2010), JGJ 138 (2016), EN 1994-1-1 (2004)) needs to be assessed for their accuracy in predicting the axial load bearing capacity of CFSTC columns. Few of the previous studies on CFSTC sections are discussed:

Rahnavard et al. (2022a, 2022b) assessed the compressive performance of closed built-up CFS columns filled with concrete experimentally and numerically. Results were utilized to check the relevance of EN 1994-1-1 codal provision for the estimation of the CFSTC columns buckling resistance. Recommendations were given by the authors for evaluating the effective cross-sectional areas of Class 4 sections, by considering various parameters.

Chen et al. (2023) investigated 42 short CFSTC columns with fixed-end boundary conditions. The experimentally obtained axial strengths were utilized to verify the accuracy of ACI 318 (2014). The comparison showed that the ACI 318 provides inaccurate estimations.

Teoh et al. (2023a) performed experimental investigation on 24 CFSTC columns filled with lightweight concrete subjected to compression. Cross-section and grade of concrete were the different parameters considered in the study. Obtained test results were adopted to verify the accuracy of design formulae's in various codal provisions (AS/NZS 2327 (2017), ANSI/AISC 360-16 (2016), EN 1994-1-1 (2004)). Teoh et al. (2023b) performed studies of the buckling performance of self-compacting lightweight concrete (LWSCC)-filled CFSTC columns. Sixteen filled columns and four hollow columns were tested considering different parameters such as member relative slenderness's ratios, concrete strengths and cross-section sizes.

2 Experimental Campaign

Nine full-scale experiments have been performed in the present study to investigate the buckling behaviour, load-deformation curve and ultimate strength of CFSTC sections. Subsequent section discusses about the taken up experimental investigation in this study.

2.1 Specimen details

Table 1 discusses about the tested specimen's details. Seven specimens have been tested to assess their performance under compression. The specimens were fabricated using four CFS U-sections assembled together using self-drilling screws to form closed square box sections. The thickness of the CFS U-sections was 1.2 mm. Fig. 1 shows the cross-section and elevation of the typical CFSTC specimen, where a is the screw spacing (100 and 150mm).

2.2 Infilled-concrete details

Three standard concrete cubic (of 150 mm \times 150 mm \times 150 mm dimensions) tests were tested to obtain the material properties of concrete. The test on the concrete cubes was conducted as per IS 456 (2000) for concrete compression testing. Table 2 summarizes, mean concrete compressive strength.

2.3 Imperfection measurements

Geometric imperfection was also measured using the laser displacement based test up shown in Fig. 2 (a and b) of the CFS C-sections used for fabricating the built-up box sections with different screw spacing which is later filled with concrete of various grades for specimen preparation.

Measured imperfections of the 5 typical CFS sections normalized to the base metal thickness has been reported in Table 3 which may be further adopted by researchers for numerical modelling of CFSTC sections.

Table 1. Specimen configuration details

Test Number	Specimen	Sheathing details
1.	CFSTC_1	CFS unfilled hollow section with 100mm screw spacing
2.	CFSTC_2	CFS unfilled hollow section with 150mm screw spacing
3.	CFSTC_3	CFSTC section with M40 concrete and 100 mm screw spacing
4.	CFSTC_4	CFSTC section with M40 concrete and 150 mm screw spacing
5.	CFSTC_5	CFSTC section with M30 concrete and 100 mm screw spacing
6.	CFSTC_6	CFSTC section with M30 concrete and 150 mm screw spacing
7.	CFSTC_7	CFSTC section with M20 concrete and 100 mm screw spacing
8.	CFSTC_8	CFSTC section with M20 concrete and 150 mm screw spacing

9.	CFSTC_9	CFSTC section with M20 concrete and 150 mm screw spacing without clamps
----	---------	---

2.4 CFS coupon test details

CFS coupon was tested as per IS 1608 (2005) for obtaining mechanical properties of the CFS used for fabricating the CFSTC sections.

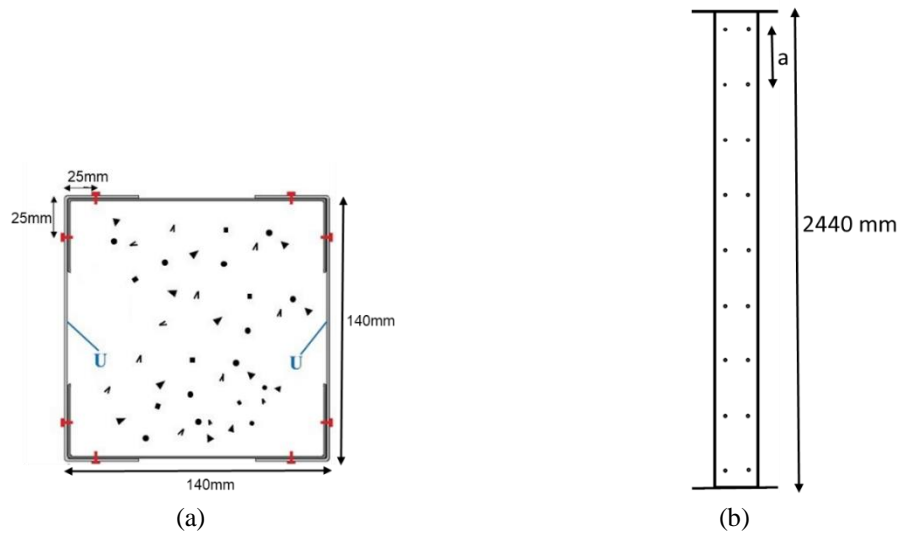
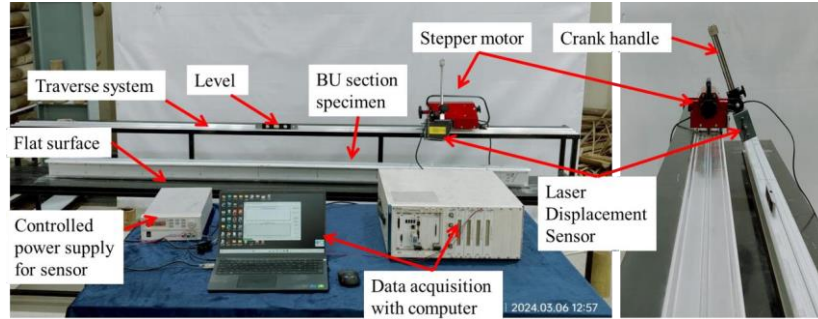


Fig. 1. Specimens considered for testing (a) cross-section; and (b) elevation of the CFSTC specimen.

Table 2. Test results of the concrete cube samples.

S.No.	Test Name	Specimen	$f_{ck,cube}$			
			Sample 1	Sample 2	Sample 3	Average
1		M20	28.59	29.65	30.25	29.49
2		M30	39.92	42.10	41.19	41.07
3		M40	51.23	52.56	52.8	52.19



(a)

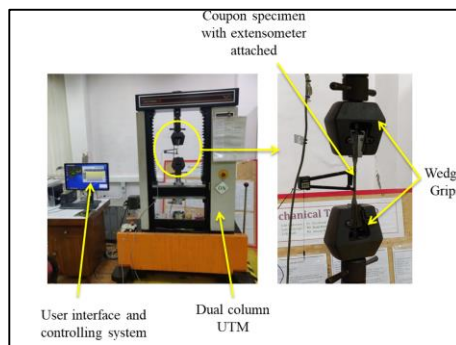


(b)

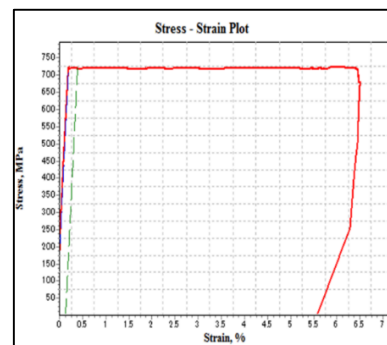
Fig 2. Details of imperfection measurement (a) imperfection measuring set-up; (b) laser displacement sensor used for measuring imperfection;

Table 3. Normalized Maximum Measured Geometric Imperfection

S. No.	Specimens	Maximum Measured Geometric Imperfection
1.	CFS U-section-1	1.63
2.	CFS U-section-2	1.36
3.	CFS U-section-3	1.98
4.	CFS U-section-4	2.19
5.	CFS U-section-5	1.78



(a)



(b)

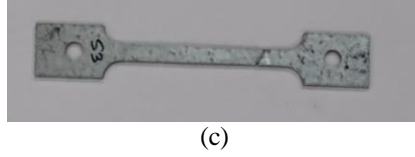


Fig. 3. CFS coupon test (a) 10 ton UTM used for the test; (b) stress–strain curve; and (c) tested CFS coupon.

2.5 Experimental test set-up for compression

300 ton UTM in the Structural Laboratory, CBRI, Roorkee, India is utilized for performing the test. As shown in Fig. 4(a). MS clamps were used for fixing the CFSTC sections at both the ends to fix the specimen at the top and bottom of the specimen [Fig. 4(b)]. Axial displacement was applied at a rate of 0.5 mm/min.



Fig. 4. (a) Experimental test set-up for axial load testing of CFSTC sections; and (b) boundary end conditions for CFSTC sections at the top and bottom respectively.

3 Experimental results and discussion

Table 4 shows the ultimate axial strength of the CFSTC specimens considered for testing in the present study.

4 Analytical Studies

According to EN 1994-1-1 (2004), the plastic resistance ($P_{pl,Rd}$) of the CFSTC specimens may be calculated using Eqs. (1-12), which takes into account the plastic resistance of the steel tube section, concrete infill, and steel reinforcement.

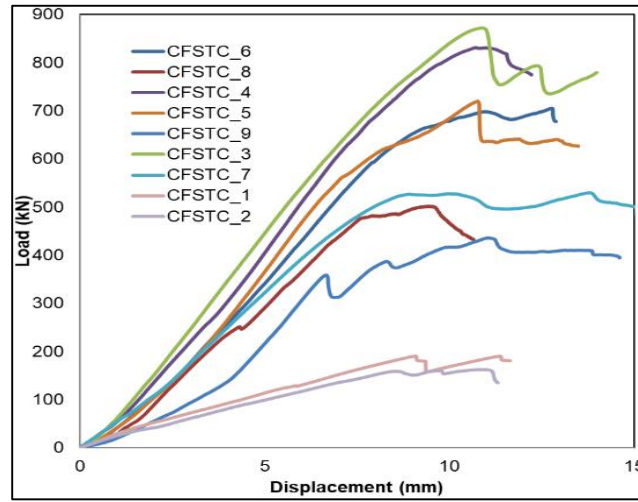


Fig. 5. Load vs. displacement curve of the tested CFSTC specimens

Table 4. Ultimate strength of the tested CFSTC specimens

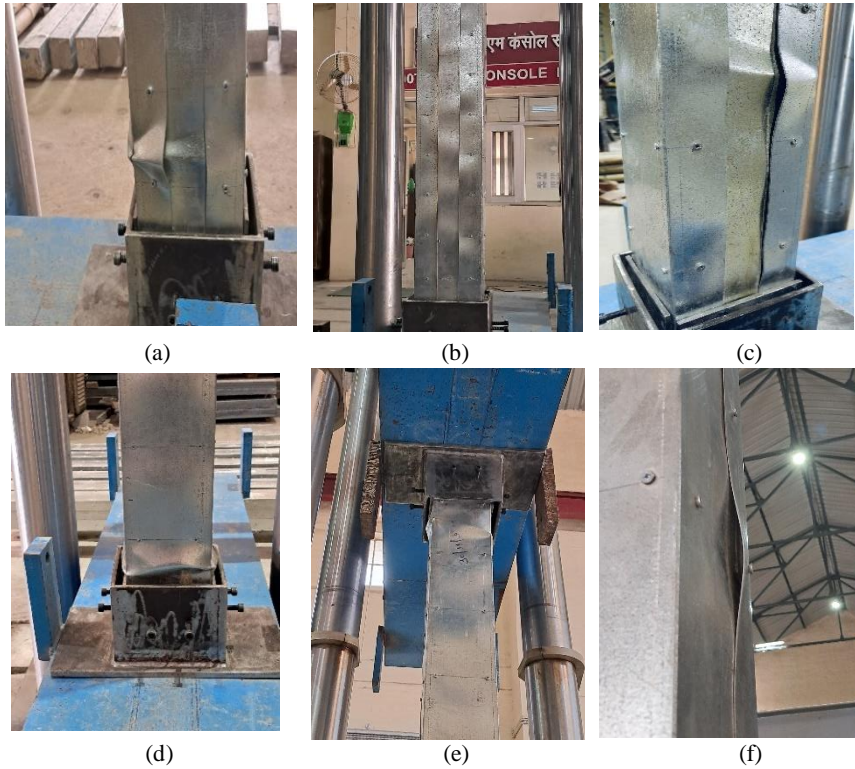
S. No.	Specimens	Ultimate axial strength (in kN)
1.	CFSTC_1	190.45
2.	CFSTC_2	162.40
3.	CFSTC_3	872.02
4.	CFSTC_4	831.40
5.	CFSTC_5	719.99
6.	CFSTC_6	705.22
7.	CFSTC_7	529.59
8.	CFSTC_8	502.06

Fig. 5 shows the experimentally obtained load vs. axial displacement curves. One of the samples CFSTC_9 failed prematurely as shown in Fig. 5. This particular test did not include clamping devices, which led to the premature collapse. Further comparisons did not take this test result into account.

The highest axial load-bearing capacity of 872.02kN was obtained for the CFSTC-3 specimens because of the highest concrete strength and lesser screw spacing of 100mm. For the CFSTC-4, CFSTC-5, CFSTC-6, CFSTC-7, and CFSTC-8 specimens, the axial load-bearing capability was 831.40kN, 719.99kN, 705.22kN, 529.59kN and 502.06kN respectively.

Fig. 6 shows the failure patterns of the various specimens considered for testing in the present study. The results for all specimens show that the deformation of the columns was representing local buckling (global buckling was not observed). Fig. 6 (a) shows the tearing of the CFS U-section in CFSTC_3 specimen at corner. Fig. 6 (b) shows local buckling waves observed near peak load in CFSTC_3 specimen. Fig. 6 (c) shows local buckling observed in CFSTC_4 specimen near the bottom.

Fig. 6 (d and e) local observed near the bottom and top clamps in CFSTC_6 specimen respectively. Fig. 6(f) shows the screw breakage observed in CFSTC_8 specimen and Fig. 6 (g and h) local buckling and web bulging observed in CFSTC_8 specimens. Local buckling was observed in CFSTC 1 near top clamp as shown in Fig. 6 (g).



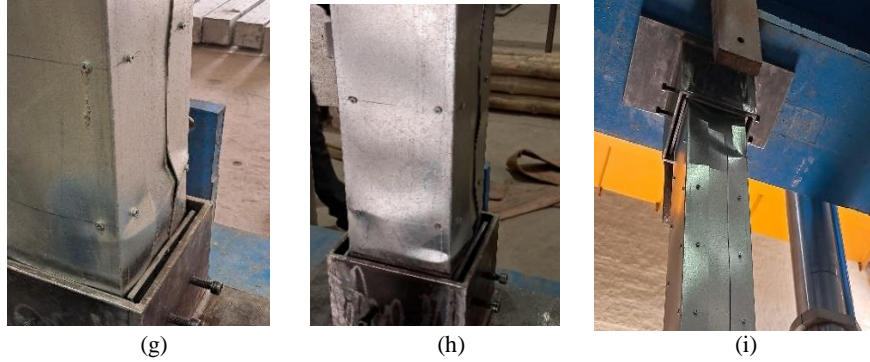


Fig. 6. Failure patterns observed in various specimens (a and b) CFSTC_3; (c) CFSTC_4; (d and e) CFSTC_6; (f to h) CFSTC_8; and (i) CFSTC_1.

Various researchers have adopted the EN 1994-1-1 (2004) for predicting the axial load carrying capacity of concrete-filled steel tubular columns (Rahnavard et al. (2022a, 2022b)). Efficacy of the EN 1994-1-1 (2004) in predicting the strength of concrete-filled steel tubular columns may be observed by the results reported in Table 5 by Rahnavard et al. (2022a).

$$N_{pl,Rd} = A_a f_{yd} + 0.85 A_c f_{cd} + A_s f_{sd} \quad (1)$$

$$N_{pl,Rd,1} = A_a f_{yd} + 0.85 A_c f_{cd} \quad (2)$$

$$N_{pl,Rd,2} = A_a f_{yd} + A_c f_{cd} \quad (3)$$

$$\delta = \frac{A_a f_{yd}}{N_{pl,Rd}} \quad (4)$$

$$N_{b,Rd,n} = \chi N_{pl,Rd,n} \quad (5)$$

$$\chi = \frac{1}{\Phi + \sqrt{\Phi^2 - \lambda^2}} \quad (6)$$

$$\Phi = 0.5[1 + \alpha(\lambda - 0.2) + \lambda^2] \quad (7)$$

$$\lambda = \sqrt{\frac{N_{pl,Rd}}{N_{cr}}} \quad (8)$$

$$N_{cr} = \frac{\pi^2 (EI)_{eff}}{L_e^2} \quad (9)$$

$$EI_{eff} = E_a I_a + k_e E_{cm} I_c \quad (10)$$

$$EI_{eff} = E_a I_a + k_e E_{c,eff} I_c \quad (11)$$

$$EI_{c,eff} = E_{cm} \frac{1}{1 + (\frac{N_{G,Ed}}{N_{Ed}}) \varphi_t} \quad (12)$$

where, $N_{pl,Rd}$ - composite columns' plastic resistance, δ - steel contribution, $N_{b,Rd}$ - design buckling resistance of a composite, χ - the column reduction factor, α - imperfection factor determined following EN 1993-1-1, λ - relative slenderness, L_e - effective length of the column, I_a and I_c - second moments (structural steel section / uncracked concrete section), k_e - correction factor and φ_t - creep coefficient.

Table 5. Normalized Maximum Measured Geometric Imperfection

S. No.	Specimens	$P_{u,test}$ (kN)	$P_{u,test}/N_{b,Rd,1}$	$P_{u,test}/N_{b,Rd,2}$	$P_{u,test}/N_{b,Rd,3}$	$P_{u,test}/N_{b,Rd,4}$
	$R-2C+2U-1$	498.59	0.81	0.77	1.08	1.00
	$R-2C+2U-2$	486.53	0.79	0.75	1.05	0.98
	$R-2C+2U-3$	462.66	0.76	0.72	1.00	0.93
Mean Value			0.78	0.75	1.04	0.97
Standard Deviation			0.03	0.02	0.04	0.037
Coefficient of Variation (%)			3.79	3.79	3.79	3.79

5 Conclusions

The axial behaviour of concrete-filled cold-formed steel columns (CFSTC) columns was investigated in the present study. An experimental program consisting of 9 CFSTC column specimens of three different concrete grades and two different screw spacing's used for connecting the CFS U-section to form the CFSTC sections. The experimental program encompassed material tests, fresh concrete properties tests, initial global geometric imperfection measurements and pin-ended column tests. The mechanical behaviours including failure modes, lateral deflections, flexural buckling resistances, load-end shortening relationship were reported and discussed. The following summarizes the findings:

1. The experimental results showed the following axial load capacities of 831.40kN, 719.99kN, 705.22kN, 529.59kN and 502.06kN for the CFSTC-4, CFSTC-5, CFSTC-6, CFSTC-7, and CFSTC-8 specimens, the respectively.
2. Local buckling was major failure mode observed in all the specimens, screw breakage only occurred in CFSTC_8 specimen having screw spacing of 150mm, therefore 100mm screw spacing is recommended.
3. Clamping device restricted the premature failure of the CFSTC specimens and lead to proper distribution of the load at the top of the specimens.
4. The obtained experimental axial capacities will be compared with the predicted axial capacity values derived from EN 1994-1-1 for assessing its efficacy.

References

1. ACI318, Building Code Requirements for Structural Concrete and Commentary. ACI 318-14, American Concrete Institute, Farmington Hills, Michigan, USA, 2014.
2. ANSI/AISC 360-05, Specification for Structural Steel Buildings, American Institute of Steel Construction; Chicago (IL, USA), 2005.
3. BD-032. AS/NZS 2327: Composite structures—composite steel-concrete construction in buildings. Standards Australia; 2017.

4. Chen, M. T., Zhang, T., & Young, B. (2023). Behaviour of concrete-filled cold-formed steel built-up section stub columns. *Thin-Walled Structures*, 187, 110692.
5. Committee on Specifications. ANSI/AISC 360-16: Specification for structural steel buildings. Chicago, Illinois: American Institute of Steel Construction; 2016.
6. DBJ/T 13-51-2010, Technical Specification for Concrete-Filled Steel Tubular Structures, The Department of Housing and Urban–Rural Development of Fujian Province, Fuzhou (China), 2010.
7. Eurocode 4. Design of Composite Steel and Concrete Structures, Part 1.1: General Rules and Rules for Building. BS EN 1994-1-1: 2004, British Standards Institution; London (UK), 2004.
8. IS (Indian Standard), Metallic Materials—Tensile Testing at Ambient Temperature. IS 1608, IS, New Delhi, India, 2005.
9. IS 456-2000, Plain and Reinforced Concrete - Code of Practice (Fourth Revision).
10. JGJ 138-2016, Code for Design of Composite Structures, Ministry of Housing and Urban–Rural Development of the People’s Republic of China, China, 2016, (in Chinese).
11. Rahnavard, R., Craveiro, H. D., Lopes, M., Simões, R. A., Laím, L., & Rebelo, C. (2022a). Concrete-filled cold-formed steel (CF-CFS) built-up columns under compression: Test and design. *Thin-Walled Structures*, 179, 109603.
12. Rahnavard, R., Craveiro, H. D., Simões, R. A., Laím, L., & Santiago, A. (2022b). Buckling resistance of concrete-filled cold-formed steel (CF-CFS) built-up short columns under compression. *Thin-Walled Structures*, 170, 108638.
13. Shanmugam, N. E., & Lakshmi, B. (2001). State of the art report on steel–concrete composite columns. *Journal of constructional steel research*, 57(10), 1041-1080.
14. Standards Australia, Bridge Design, Part 6: Steel and Composite Construction. AS 5100.6-2004, Sydney (Australia), 2004.
15. Tao, Z., Wang, Z. B., & Yu, Q. (2013). Finite element modelling of concrete-filled steel stub columns under axial compression. *Journal of constructional steel research*, 89, 121-131.
16. Teoh, K. B., Chua, Y. S., Dai Pang, S., & Kong, S. Y. (2023a). Experimental investigation of lightweight aggregate concrete-filled cold-formed built-up box section (CFBBS) stub columns under axial compression. *Engineering Structures*, 279, 115630
17. Teoh, K.B., Chua, Y.S., Dai Pang, S. and Kong, S.Y.(2023b). Experimental investigation of flexural buckling behaviour of self-compacting lightweight concrete-filled cold-formed built-up box section (CFBBS) columns. *Thin-Walled Structures*, 187, p.110751.
18. Uy, B., Tao, Z., & Han, L. H. (2011). Behaviour of short and slender concrete-filled stainless steel tubular columns. *Journal of Constructional Steel Research*, 67(3), 360-378.
19. Wang, F., Young, B., & Gardner, L. (2020). Compressive behaviour and design of CFDST cross-sections with stainless steel outer tubes. *Journal of Constructional Steel Research*, 170, 105942.